

The yeast *HML* I silencer defines a heterochromatin domain boundary by directional establishment of silencing

Xin Bi, Miriam Braunstein,* Gan-Ju Shei,[†] and James R. Broach[‡]

Department of Molecular Biology, Princeton University, Princeton, NJ 08544

Edited by Gary Felsenfeld, National Institutes of Health, Bethesda, MD, and approved August 10, 1999 (received for review June 22, 1999)

The eukaryotic genome is divided into functional domains defined in part by local differences in chromatin structure and delimited in many cases by boundary elements. The *HML* and *HMR* loci in the yeast *Saccharomyces cerevisiae* are transcriptionally silent chromosome domains. Each locus is bracketed by two cis-acting sequences, designated E and I, that serve to establish and maintain repression of genes within each locus. We show that repression at *HML* is uniformly high between E and I but decreases sharply beyond I. The region of repression at *HML* generally correlates with the domain of histone hypoacetylation. Despite the sharp definition of the boundaries of *HML*, no sequence capable of blocking the spread of heterochromatin resides in the sequences flanking *HML*. We find, though, that inverting the orientation of I increases silencing outside of *HML* while weakening silencing within *HML*. These results indicate that the *HML* I silencer establishes a boundary between active and inactive chromatin at *HML*, but does so by organizing inactive chromatin in only one direction. This represents a different mechanism for delimiting the boundaries of a eukaryotic chromosome domain.

The eukaryotic genome is divided into domains of distinct regulatory potential. The same gene inserted into different sites in the *Drosophila* or mammalian genome can exhibit markedly different levels of expression (reviewed in ref. 1). This position effect on gene expression likely reflects local differences in chromatin structure as well as the particular distribution of enhancers and other regulatory elements throughout the genome. One question posed by the existence of different domains is how these local differences in expression potential are restricted to limited regions of the genome.

Studies of specific regions of the *Drosophila* and vertebrate genomes suggest that, at least for some domains, the regulatory potential of that domain is precisely delimited by boundary or insulator elements that serve to restrict the effects of transcriptional activity to the region lying between pairs of such elements. Two small segments, *scs* and *scs'* (specialized chromatin structure), flank the 87A7 hsp70 heat shock locus of *Drosophila* and serve to limit the effects of heat shock activation to the locus (2, 3). These segments can function as nonspecific boundary elements: when bracketing a transgene they insulate it from position-effect variegation and when placed between an enhancer and a promoter either segment can block transcriptional activation of the promoter by the enhancer. The *scs* and *scs'* elements contain binding sites for the *zw5* protein (M. Gaszner and P. Schedl, personal communication) and the BEAF-32 protein (4), respectively. A cluster of binding sites for the suppressor of hairy wing [*su(Hw)*] protein constitute a second boundary element in *Drosophila* (5).

A DNase I hypersensitive site (5'HS4) from the chicken β -globin locus also exhibits boundary activity (6). This element resides at the transition between active chromatin of the β -globin locus, as marked by both DNase I sensitivity and high levels of histone acetylation, and the adjacent inactive chromatin domain. The 5'HS4 element can insulate transgenes from position-effect variegation and can function in *Drosophila* to block enhancer-

mediated activation of an adjacent promoter. Thus, although the molecular mechanism of insulation is not yet resolved, these studies clearly demonstrate that at least some regulatory domains are restricted by the activity of specific boundary elements.

Examples of chromosome domains in the yeast *Saccharomyces cerevisiae* include the homothalic mating type loci, *HML* and *HMR*, as well as telomeres. Genes present at the expressed *MAT* locus on chromosome III determine the mating type of a haploid yeast cell. Identical mating type genes also exist at the *HML* or *HMR* loci on the same chromosome. However, at these loci, the mating type genes are not expressed, even though all the signals for expression are present (reviewed in ref. 7). Ectopic genes inserted at the *HM* loci are also subject to repression, indicating that this is a region-specific but gene-nonspecific event. This repression, known as silencing, results from the formation of a heterochromatin-like chromatin structure across the loci (reviewed in ref. 8). A heterochromatin-like structure also exists in sequences close to the telomeres in yeast, which causes transcriptional silencing of genes inserted near the telomeres.

Establishing and maintaining repression at the *HM* loci require a number of trans-acting factors and two cis-acting sites, named silencers, flanking each *HM* locus. Silencers are small (<250 bp) sequences composed of various combinations of binding sites for DNA binding proteins—Rap1, Abf1, and the origin recognition complex—whose binding are required for silencing (Fig. 1A). A variety of other proteins, including Sir1 through Sir4 and histones H3 and H4, are also required for transcriptional silencing (7). The extensive interactions among the trans-acting factors support the current model for silencing in which the silencer-binding proteins and Sir1 recruit a complex of Sir2, Sir3, and Sir4 to the silencer, which then extends along the neighboring nucleosomes, serving as an integral part of the silent chromatin (9).

The fact that repressive chromatin emanates outward from a silencer raises the question of what prevents the repressive chromatin from extending indefinitely. Do boundary elements around the silent *HM* loci actively block the spread of heterochromatin elicited by silencers, or does silencing simply decay stochastically as a function of distance from the silencers? Recent studies revealed that certain sequences surrounding the *HMR* locus have the ability to block the spread of silencing from *HMR* (10). In two other independent studies, UASrpg, consisting of multiple binding sites of Rap1, and sequences containing

This paper was submitted directly (Track II) to the PNAS office.

Abbreviation: 5-FOA, 5-fluoro-orotic acid.

*Present address: Department of Microbiology and Immunology, Albert Einstein School of Medicine, New York, NY 10461.

[†]Present address: Merck and Company, Rahway, NJ 07065.

[‡]To whom reprint requests should be addressed. E-mail: jbroach@molecular.princeton.edu.

The publication costs of this article were defrayed in part by page charge payment. This article must therefore be hereby marked "advertisement" in accordance with 18 U.S.C. §1734 solely to indicate this fact.

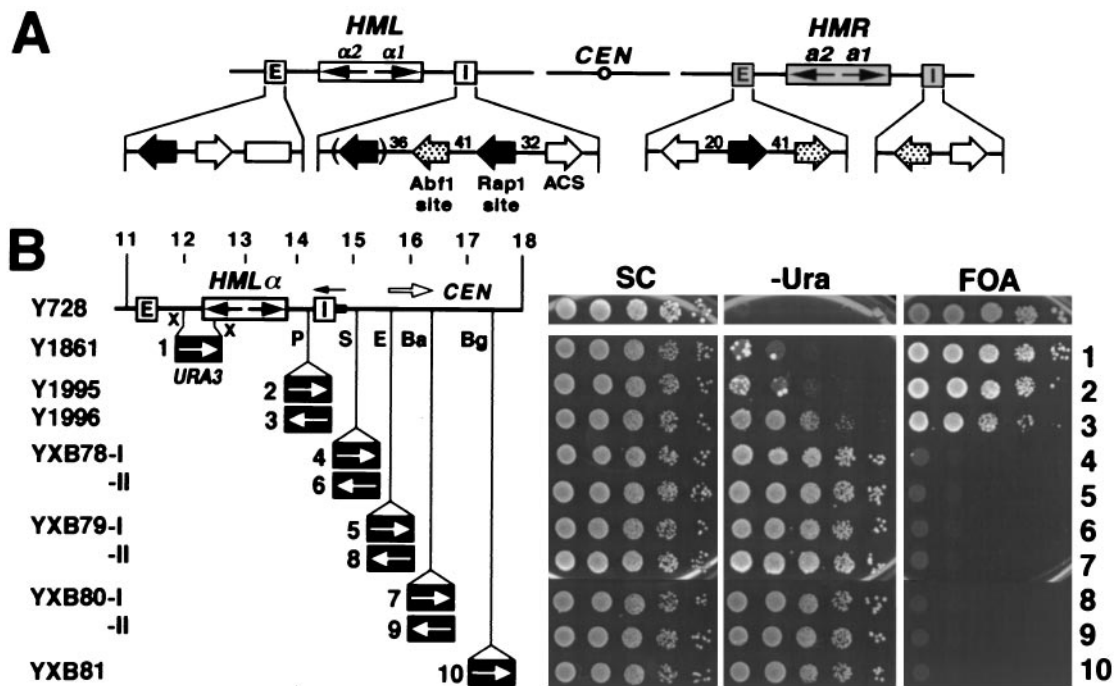


Fig. 1. Transcriptional silencing is uniformly high within *HML* but sharply decreases beyond the I silencer. (A) Schematic representation of the *HML* and *HMR* loci and their silencers on chromosome III. *CEN*, centromere. The open box in the *HML* E silencer represents the D-element (29). (B) The pattern of transcriptional silencing within and near *HML*. (Left) Strains used. The 11- to 18-kb fragment of chromosome III, including *HML*, is shown. The *HML* I silencer (I in open box) corresponds to position 14561–14701 (22). The filled bar to the right of *HML* I is 14702–14838. *URA3* replaces 12015–12535 (*Xba*I–*Xba*I) in Y1861. Strains Y1995–YXB81 have *URA3* inserted at the *Pvu*II (P, 14441), *Sna*BI (S, 15016), *Eco*RV (E, 15410), *Bam*HI (Ba, 16263), and *Bgl*II (Bg, 17344) sites, respectively, in both orientations. Copies of *URA3* in these strains are designated 1–10, according to the positions of the *URA3* promoter relative to *HML* I. X, *Xba*I site. (Right) Growth phenotypes. Cells of each strain were grown to late logarithmic phase, and serial dilutions (10-fold) were spotted on test plates and allowed to grow for 3 days. SC, synthetic complete medium; –Ura, SC medium lacking uracil; FOA, SC medium containing 5-fluoroorotic acid (5-FOA).

multiple Reb1 and/or Tbf1 binding sites have both been identified as heterochromatin boundary elements in yeast (11, 12).

In this study, we defined the transcriptionally silent domain across the *HML* locus and tested for the presence of functional boundary elements surrounding the locus. We show that silencing is uniformly high within the region bracketed by the E and I silencers but sharply decreases beyond the I silencer. Unlike the situation for *HMR*, sequences surrounding the *HML* locus exhibit no detectable boundary activity. However, we found that inverting the I silencer extended silencing beyond I but diminished silencing within *HML*. These data, together with our previous finding that certain silencers promote ectopic silencing in only one orientation (13), suggest that *HML* silencers delimit a repression domain by unidirectional establishment of silencing.

Materials and Methods

Plasmids and Strains. The plasmids described below were constructed by inserting a sequence of chromosome III into the polylinker of pUC19. Plasmid pUC26 contains the *Bam*HI–*HML*–*Bam*HI fragment corresponding to region 9666–16263 of chromosome III (base pair coordinates are from the complete sequence of chromosome III). The *Hpa*I–*HML* I–*Hind*III (14561–14838) fragment in plasmid pUC26 was inverted to make plasmid pXB87. Plasmids pMB35, pAR61, pMB11, pMB10, and pDM33 contain the *Hind*III–*Hind*III (13679–14838), *Hind*III–*Bam*HI (14838–16263), *Eco*RI–*Hind*III (14838–16713), *Hind*II–*Hind*III (17021–18961), and *Xba*I–*Xba*I (10838–12015) fragments, respectively. The *Hpa*I–*HML* I–*Hind*III fragment (14561–14838) was inserted at *Hpa*I site of pDM33 in both orientations to yield plasmids pGJ51 and pGJ52. The 1.1-kb *Bgl*II–*URA3*–*Bgl*II fragment of plasmid pFL44 (14) was used in constructing a series of plasmids for the insertion of *URA3* at

different sites within or near the *HML* locus on chromosome III. *URA3* was inserted at the *Pvu*II site of pMB35 in both orientations to make plasmids pMB36 and pMB37, at *Sna*BI of pAR61 to make plasmids pMB16a and -b, at the *Eco*RV site of pAR61 to generate plasmids pMB22a and -b, at the *Bam*HI site of pMB11 to make plasmids pMB13a and -b, and at the *Bgl*II site of pMB10 to make plasmids pMB12a and -b. Plasmid pGJ8 contains the *Eco*RI–*Hind*III (11294–14838) fragment of chromosome III in which the *Xba*I–*Xba*I (12015–12535) fragment was replaced by *URA3*. Plasmid pMB21 consists of pRS404 (15) into which the *SIR3* and *SUP4-o* genes have been inserted at the *Sac*I + *Bam*HI and *Bam*HI sites, respectively. Plasmids pXB68, pXB69, pXB70, and pXB71 contain PCR fragments from chromosome III positions 9658–11158 (designated α , Fig. 4A); 14701–16201 (β); 289,776–291,276 (γ); and 293,628–295,128 (δ), respectively, inserted at the *Spe*I site of pYXB26 (11).

Strain Y851 is *mata1 HML α HMR α leu2–3,112 trp1 Δ ade8 ura3–52*, and strain Y1423 is identical to strain Y851 except for inactivation of *SIR3* by insertion of *LEU2*. All other strains used in this study were derived from strain DMY1 (*MATA ura3–52 leu2–3,112 ade2–1 lys1–1 his5–2 can1–100*; ref. 16). Strain YXB76 was made by transforming strain DMY20 (DMY1, $\Delta E::SUP4-o-HML\alpha-\Delta I$; ref. 16) to canavanine-resistance with the *Bam*HI–E–*HML\alpha*–I(inverted)–*Bam*HI fragment of plasmid pXB87. Strain YXB77 was derived from strain YXB76 by disrupting *SIR3* with *LEU2* as described (16). Strain Y1861s was constructed by transforming strain DMY2 (DMY1, *sir3::LEU2*; ref. 16) to Ura⁺ with *Eco*RI plus *Hind*III-digested pGJ8 DNA. Strains Y1995s, Y1996s, YXB78-Is, YXB78-IIs, YXB79-Is, YXB79-IIs, YXB80-Is, YXB80-IIs, and YXB81s were similarly derived from DMY2 by transformation with appropriately digested pMB36, pMB37, pMB16a, pMB16b, pMB22a, pMB22b,

pMB13a, pMB13b, and pMB12a DNAs, respectively. These strains were rendered *SIR*⁺ by integrating pMB21 at *TRP1* in the genome, resulting in the strains listed in Fig. 1B. All the strains listed in Fig. 5A were obtained by first transforming strain YXB77 to Ura⁺ with the plasmids listed above and then converting the resulting transformants to *SIR*⁺ by integrating pMB21 at *TRP1* in the genome. Strains YXB68 to YXB71 were made by transforming strain Y2047b (DMY1, $\Delta E::SUP4-o-HML\alpha-\Delta I$ *LEU2-GAL10-FLP1* [*cir*⁰]; ref. 17) to canavanine-resistance with *Bam*HI-digested plasmid pXB68 to pXB71, respectively. Strain DMY19s (DMY1, $\Delta E::SUP4-o-HML\alpha-\Delta I$ *sir3::LEU2*) was transformed to canavanine-resistance by using *Xba*I-digested pGJ51 or pGJ52 to yield strains GJY75s and GJY77s, which were transformed with pMB21 to yield strains GJY75 and GJY77. Strain YXB100 is DMY1, *E-HML α - ΔI sir3::LEU2 SIR3-SUP4-o*. All strain constructions were confirmed by Southern blot analysis.

Chromatin Immunoprecipitation. Chromatin immunoprecipitation assays were performed as described previously (18).

Results

Transcriptional Silencing Is Uniformly High Within *HML* but Sharply Decreases Beyond the *I* Silencer. The *URA3* gene provides a convenient reporter for studying transcriptional silencing. *URA3* expression can be assessed by cell viability assays on medium containing 5-fluoroorotic acid (5-FOA) or on medium lacking uracil. The *URA3* gene product converts the drug 5-FOA to a toxic metabolite, so that cells with basal level expression of *URA3* are sensitive to 5-FOA, whereas *ura3* cells or cells in which *URA3* expression is repressed below basal level can grow on 5-FOA medium (19). Depletion of uracil from the medium activates the Ppr1 transactivator, which in turn binds to the upstream activating sequence (UAS) of *URA3* and increases expression of the gene. Therefore, while cell growth on 5-FOA medium indicates repression of the basal level of transcription of *URA3*, growth on uracil minus (-Ura) medium reflects the ability of the cell to activate expression of *URA3*. Telomeric silencing can repress basal expression but not the activated expression of *URA3* mediated by Ppr1 (20). In contrast, *HM* silencing represses both basal and activated *URA3* expression (see below).

To define the domain of transcriptional repression associated with the silent *HML* locus, we first examined the extent of repression of *URA3* inserted at various locations between the silencers (Fig. 1B). Viability assays on 5-FOA medium indicated that basal expression of *URA3* was repressed in these strains: the 5-FOA-resistant fraction of cells from each strain was essentially equivalent to that of a *ura3* strain (Y728). Viability assay on -Ura medium also showed significant repression of activated expression of *URA3* within *HML* (Y1861 and Y1995), except for *URA3* in Y1996, whose promoter is located only \approx 110 bp from *I*. In summary, within the *HML* locus, silencing of both basal and activated transcription of *URA3* is, in general, uniformly high. The slightly diminished silencing of activated transcription of *URA3* in Y1996 likely results from the unique chromatin context near *I* attributable to the occupancy by silencer-binding proteins. This is supported by evidence presented below.

We next examined transcriptional repression in the region immediately adjacent to *HML*. We inserted the *URA3* gene at various sites centromere-proximal to *HML I* and then assessed its basal and activated levels of expression (Fig. 1B). In these experiments and those above, we integrated all the *URA3* reporter genes into a *sir3*⁻ strain and only subsequently converted the strains to *SIR*⁺ (see *Materials and Methods*). This precluded inadvertently selecting activated, or silencing resistant, reporter genes in the course of strain construction. Data presented in Fig. 1B indicate that neither basal nor activated

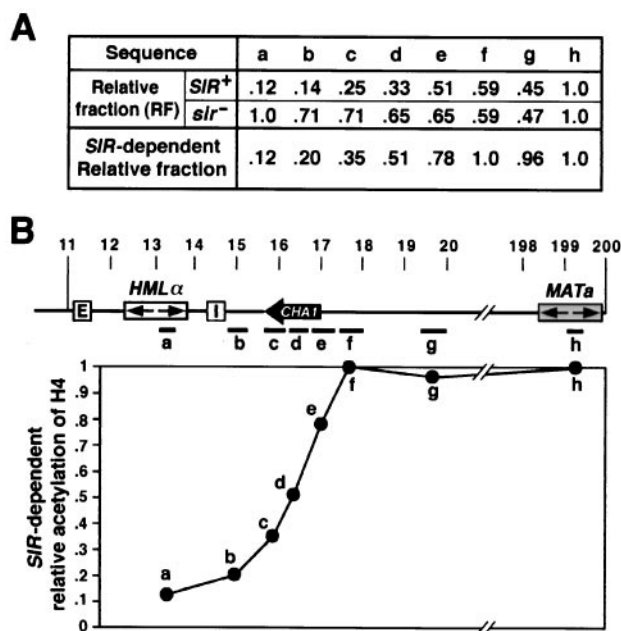


Fig. 2. The domain of histone H4 hypoacetylation at *HML*. (A) Relative fraction of different sequences within and adjacent to *HML* immunoprecipitated with anti-acetylated histone H4 Ab. See text for calculations. (B) *SIR*-dependent relative acetylation of histone H4 as a function of position on chromosome III. (Upper) Schematic representation of the 11- to 200-kb sequence of chromosome III analyzed in the chromatin immunoprecipitation assay. The *HML α* and *MATa* loci and the *CHA1* gene are indicated. Various DNA sequences (coordinates in parentheses) used to make probes for slot blot analysis are: a (13172–13418), b (14839–15360), c (15730–16264), d (16264–16714), e (16714–17562), f (17562–18049), g (19574–20029), and h, the *MATa*-specific probe (16). (Lower) *SIR*-dependent relative acetylation of histone H4 described in A, plotted as the function of the positions of the a–h probes.

expression of *URA3* in strains YXB78–81 is repressed. Note that *URA3* in strain YXB78-I resides very close (300 bp centromere-proximal) to *I* and yet is not silenced. The loss of silencing potential immediately outside the *I* site suggests that *I* or sequences in the vicinity of *I* constitute a boundary for the silent chromatin domain across *HML*.

The Domain of Histone Hypoacetylation Correlates with the Domain of Transcriptional Repression at *HML*.

Histones H3 and H4 in nucleosomes constituting silent chromatin exhibit a reduced level of acetylation compared with that in nucleosomes constituting active chromatin (8, 18, 21). Accordingly, we investigated whether the domain of gene silencing across *HML* locus correlated with the pattern of chromatin hypoacetylation. To determine the extent of Sir-dependent histone H4 hypoacetylation at and around *HML*, we immunoprecipitated chromatin isolated from isogenic *SIR*⁺ (Y851) and *sir*⁻ (Y1423) strains with Abs against acetylated histone H4 (18). The presence of various sequences in or near *HML* in the immunoprecipitated chromatin was detected by slot blot hybridization of the immunoprecipitated DNA with appropriate genomic probes (Fig. 2B, a–h). The fraction of a particular sequence present in the immunoprecipitate was determined by densitometry analysis of the probed blots and normalized relative to the amount of *MAT* sequence present in the same immunoprecipitate, a value defined as the relative fraction (Fig. 2A). Consistent with previous observations, we found that DNA from within *HML* in a *SIR*⁺ strain was underrepresented in the acetylated fraction, indicating that hypoacetylated nucleosomes package the silent *HML* locus. Nucleosome hypoacetylation at *HML* was Sir-dependent, as

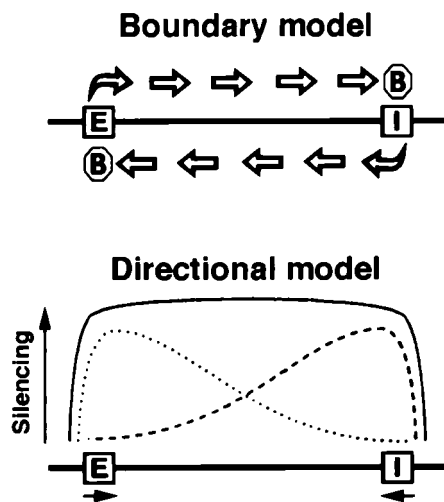


Fig. 3. Proposed mechanisms for delimiting transcriptionally silenced domains. The E and I silencers are indicated. The octagons represent putative boundary elements. See text for details.

evidenced by the fact that the equivalent amounts of *HML* and *MAT* were recovered in acetylated chromatin immunoprecipitated from a *sir3⁻* strain (Fig. 2A).

To determine the domain of hypoacetylation around *HML*, we probed the immunoprecipitates obtained with anti-acetylated histone H4 with DNA probes located at increasing distances outward from *HML* toward the centromere. As noted in Fig. 2A, the amount of DNA in the immunoprecipitate, relative to the amount of *MAT* DNA in the immunoprecipitate, increased with increasing distance from *HML* for chromatin isolated from a *SIR⁺* strain. In contrast, the relative amount of DNA in the immunoprecipitate decreased slightly with increasing distance from *HML* for chromatin isolated from a *sir⁻* strain. Accordingly, to focus on the Sir-dependent acetylation effects, we normalized the relative fraction of a sequence in the immunoprecipitate from the *SIR⁺* strain to that of the same sequence in the immunoprecipitate in the *sir⁻* strain to yield a Sir-dependent relative fraction value for each sequence (Fig. 2A). As is evident from the data, the relative acetylation level of H4 is low within *HML* (Fig. 2B, a) and increases in the centromere-proximal

region of I (Fig. 2B, b–g). The lack of a sharply defined transition in histone acetylation may be because of the limitations of the chromatin immunoprecipitation assay, in which immunoprecipitation was performed on chromatin fragments of random, variable sizes. Nonetheless, the pattern of acetylation generally corresponds with the pattern of transcriptional repression of the *URA3* gene inserted around *HML*.

The *HML* I Silencer Defines the Heterochromatin Boundary by Initiating Silencing in Only One Direction. The above experiments on the pattern of gene silencing and the profile of histone H4 acetylation around the *HML* I silencer indicate that the I silencer lies at or near the breakpoint between fully repressed and fully activated domains of gene expression. We can envision two distinct models to account for the colocalization of the breakpoint and the I silencer (Fig. 3). The “boundary model” posits elements flanking the *HML* locus that actively block the spread of silencing initiated at the silencers, as is the case for at least the rightward (telomere-proximal) side of *HMR* (10). In this model, the boundary element would lie close to the *HML* I silencer, either as a distinct element or overlapping the I site. The “directional model” proposes that no boundary elements surround *HML*. Rather, the E and I silencers would initiate silenced chromatin that would emanate outward in only one direction, but that would decay stochastically with increasing distance from the silencer. We assume that the activities of the two silencers would be additive so that repression of sequences lying between them would be uniformly high. Both models yield a domain of repression consistent with that observed at *HML*.

To distinguish between these two models, we tested whether sequences flanking *HML* were capable of protecting a promoter from the repressive effects of heterochromatin initiated at a silencer. This “blocking” assay has been used to identify and characterize other heterochromatin boundary elements in yeast (10–12). Fragments 1.5 kb in length corresponding to the flanking regions of *HML* and *HMR* were inserted between the E silencer and the α genes in the *HML* Δ I locus of strain YXB26 (Fig. 4A). The effect of each sequence on silencing of the *HML* α genes imposed by the E silencer could be determined by quantitative mating, because the mating efficiency of this *MATa* strain is inversely proportional to the level of expression of the α genes resident at *HML*. As is evident from the data in Fig. 4B, no sequences with silencer blocking activity lies within the 1.5-kb fragments flanking the *HML* locus (compare YXB68 and

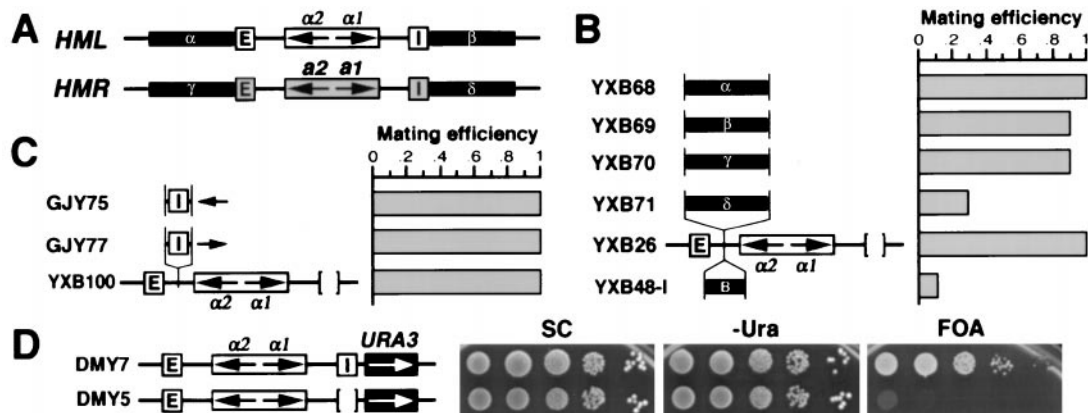


Fig. 4. Neither sequences flanking *HML* nor the *HML* I silencer actively block the spread of silencing. (A) Sequences (1.5 kb each, designated α – δ) flanking the *HML* and *HMR* loci. (B) Boundary element activity of sequences surrounding *HML* loci. YXB68–71 have the α – δ sequences inserted at *HML* Δ I of YXB26, respectively. YXB48-I has the 149-bp boundary element from the *TEF2* promoter inserted at *HML* Δ I (11). Mating efficiency of each strain was determined as described (11). Mating efficiency of YXB26 was taken as one. (C and D) The *HML* I silencer is not a boundary element. (C) Strains GJY75 and GJY77 have the I silencer inserted at the *Hapl* site of the *HML* Δ I locus in YXB100, but in opposite orientations. Mating efficiency of YXB100 was taken as one. (D) Growth phenotypes of strains DMY5 and DMY7 (16).

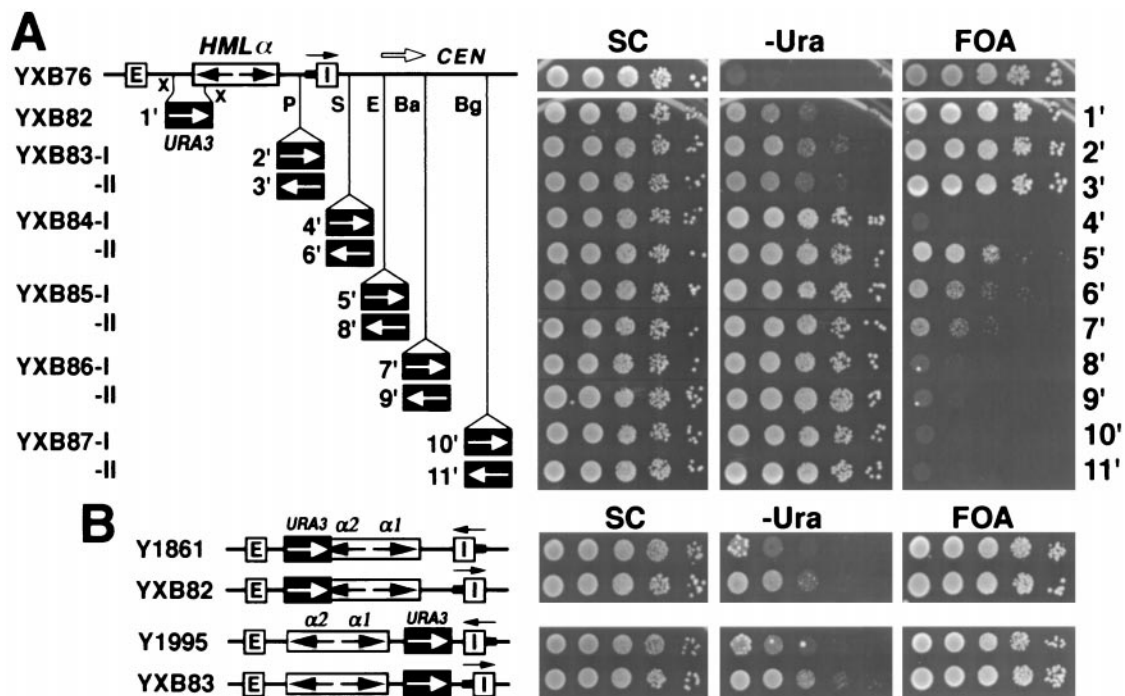


Fig. 5. The *HML* I silencer functions as a heterochromatin domain boundary by directional silencing. (A) Growth phenotypes of strains with *URA3* positioned within or centromere-proximal to *HML* when the I silencer is inverted. The strains used are the same as those in Fig. 1B, except that the *HML* I silencer plus a small region to its right (14561–14838) is inverted in each. Copies of *URA3* in these strains are designated 1'–11', according to the positions of the *URA3* promoter relative to *HML* I. (B) Effect of flipping *HML* I on silencing within *HML*. Cell growth on different media was tested as described in the legend to Fig. 1B.

YXB69 to YXB26). In contrast, the 1.5-kb sequence to the right of *HMR* I (telomere proximal) exhibits silencer blocking activity (Fig. 4, YXB71), consistent with an earlier identification of boundary activity within a 1-kb sequence encompassed by this fragment (10). Similarly, a 149-bp fragment from the *TEF2* promoter that we identified previously as possessing boundary activity (11) was also able to block repression of the *HML* α genes by silencing initiated at the E silencer (Fig. 4, YXB48-I). However, the 1.5-kb sequence from the left of *HMR* E (centromere proximal) did not exhibit blocking activity, although it overlaps ≈ 500 bp with the 1-kb leftward boundary of the *HMR* repression domain (10) (Fig. 4, YXB70). Finally, we also tested the *HML* I silencer, as defined by Feldman *et al.* (22), for silencer-blocking activity. As shown in Fig. 4C, insertion of I in either orientation between the E silencer and the α genes did not alleviate silencing of the α genes. Therefore, neither sequences surrounding the *HML* locus nor the *HML* I silencer can restrict the spread of transcriptional repression initiated at a silencer. These observations are inconsistent with the “boundary model” described above.

As a second test of the “boundary model,” we examined the effect of eliminating the I silencer on the extent of repression of a reporter gene lying immediately beyond I. If the I silencer comprises a boundary element capable of blocking the spread of heterochromatin, then deleting the I silencer should allow heterochromatin initiated at the E silencer to spread beyond the I site. This would result in increased repression of a gene lying immediately outside the I site. Accordingly, we examined the expression state of a *URA3* gene inserted 100 bp centromere-proximal to I in two isogenic strains, in one of which the I site is intact and in one of which the I site has been deleted. As seen in Fig. 4D, the level of repression of the *URA3* gene actually decreases on deletion of I, as evidenced by the fact that the *DMY5* cells were not able to grow on FOA medium. This result

adds further weight to the conclusion that the I site does not have silencer-blocking activity.

To test the “directional model,” we inverted the I silencer and examined its effect on the repression of *URA3* gene inserted at different sites within and centromere proximal to *HML* (Fig. 5A). The strains shown in Fig. 5A are identical to those in Fig. 1B, except that the *HML* I silencer is inverted in each of them. We found that inverting the orientation of I resulted in significant changes in the repression pattern of *URA3* expression in the region to the right of the I silencer. First, repression of basal transcription of *URA3* was increased such that a fraction of the cells were able to grow on 5-FOA medium (compare YXB84-II to YXB87-II in Fig. 5A with their counterparts in Fig. 1B). Second, as the distance between the *URA3* promoter and the I silencer increased, both the number and the size of the colonies on 5-FOA medium decreased, indicating that silencing diminishes with increasing distance. We noted a discontinuity in the repression pattern, in that strain YXB84-I failed to grow on FOA, indicating that the *URA3* gene inserted immediately adjacent to I was completely derepressed, whereas those inserted farther away were repressed. This is consistent with previous observations, which indicate that chromatin in the region immediately adjacent to a silencing organizing center is not repressive (23, 24). We also observed changes in silencing of activated transcription of *URA3* within *HML* (Fig. 5B). Strain Y1861 harboring *URA3* within *HML* cannot grow on –Ura medium, indicating full repression of activated *URA3* expression. However, strain YXB82 derived from Y1861 by inverting the I silencer shows limited growth on –Ura medium, indicating that inversion of I diminished repression of activated expression of *URA3*. Similar results were obtained for strains Y1995 and YXB83 (Fig. 5B). In summary, we conclude that with I in its natural orientation, silencing is strong within *HML* but weak or nonexistent in the region centromere proximal to I. Inversion of I weakens silencing within *HML* but strengthens silencing in the

centromere proximal region next to I. This is in full accordance with the “directional model.”

Discussion

The results presented in this report describe a different means of establishing a distinct chromatin domain within a eukaryotic genome. Previous studies examining the region of transition between active and inactive chromatin domains have identified elements that possess either enhancer-blocking activity or heterochromatin-blocking activity (reviewed in ref. 1). In this study, we were able to map quite precisely the transition between active and inactive chromatin on one side of the silent *HML* locus in yeast. In this case, though, we found that no sequence with the ability to block the spread of heterochromatin resides at or near this transition point. Rather, we found that the boundary appears to derive from the fact that the silencer promotes formation of heterochromatin in only one direction. Accordingly, heterochromatin forms to one side of the silencer but not to the other, effectively creating a boundary.

To account for the pattern of repression we observe at *HML*, we assume that the E and I silencers promote formation of heterochromatin that propagates inward toward the mating-type genes. We further assume that the repressive effect imposed by each silencer diminishes with increasing distance from the silencer, similar to the pattern of telomeric silencing (25–27). Finally, we assume that the repressive effects of the two silencers are additive. In this sense, our model is consistent with the concept proposed by Boscheron *et al.* (28), which states that the silencers at *HML* cooperate. However, our results reinforce the notion that such a cooperation does not represent a physical interaction between the two silencers, which would delimit silencing to the loop of DNA formed between them. This possibility is most clearly eliminated by the results presented in Fig. 4C, in which we showed that moving I to a site between E and the α mating genes does not eliminate repression of the α

genes. Finally, we previously showed that I is capable of promoting repression of genes at *MAT* only when inserted next to *MAT* and pointing toward the *MAT* genes (that is, with I oriented so that the *MAT* genes are to the same side of I as the α genes are at *HML*). Insertion of I at this same site next to *MAT* but in the opposite orientation failed to elicit repression of the *MAT* genes (13). Thus, our previous demonstration of the orientation dependence of I-mediated repression is consistent with our current hypothesis that silencing spreads outward from I at *HML* only in the direction of the α genes.

While the *HML* I and *HMR* E silencers both contain binding sites for origin recognition complex, Rap1, and Abf1 with relatively similar arrangements (Fig. 1A), they differ in strength and orientation dependence. *In vitro* binding assays have shown that the Rap1 site in *HML* I has significantly lower affinity for Rap1 than does the site in *HMR* E (28). Footprinting studies revealed a second weak, nonessential, Rap1-binding site in *HML* I (Fig. 1A, Rap1 site in parentheses; ref. 28). The affinity of origin recognition complex or Abf1 to its binding site in the two silencers has not been directly compared. The difference in the potency of silencing by *HML* I and *HMR* E silencers could reflect any combination of a number of possible factors, including the small differences in the spacing of the three protein-binding sites, the affinities of individual sites to their respective factors, or the sequence context of the sites. However, the difference in the directionality of silencing between the two silencers is more difficult to interpret. Further experiments need to address whether a single component of a silencer or the concerted action of all components is responsible for the observed directionality of the silencer and how that local structure is translated into a unidirectional initiation of heterochromatin.

We thank Dr. C. D. Allis for the gift of anti-H4 Ab and Karun Shekari for technical assistance. This work was supported by National Institutes of Health Grant GM48540 (to J.R.B.) and by Postdoctoral Fellowship PF4298 from the American Cancer Society (to X.B.).

1. Udvardy, A. (1999) *EMBO J.* **18**, 1–8.
2. Kellum, R. & Schedl, P. (1991) *Cell* **64**, 941–950.
3. Kellum, R. & Schedl, P. (1992) *Mol. Cell. Biol.* **12**, 2424–2431.
4. Zhao, K., Hart, C. M. & Laemmli, U. K. (1995) *Cell* **81**, 879–889.
5. Geyer, P. K. & Corces, V. G. (1992) *Genes Dev.* **6**, 1865–1873.
6. Chung, J. H., Whiteley, M. & Felsenfeld, G. (1993) *Cell* **74**, 505–514.
7. Laurenson, P. & Rine, J. (1992) *Microbiol. Rev.* **56**, 543–560.
8. Braunstein, M., Holmes, S. G. & Broach, J. R. (1997) in *Nuclear Organization, Chromatin Structure and Gene Expression*, eds. van Driel, R. & Otte, A. P. (Oxford Univ. Press, Oxford), pp. 250–275.
9. Lustig, A. J. (1998) *Curr. Opin. Genet. Dev.* **8**, 233–239.
10. Donze, D., Adams, C. R., Rine, J. & Kamakaka, R. T. (1999) *Genes Dev.* **13**, 698–708.
11. Bi, X. & Broach, J. R. (1999) *Genes Dev.* **13**, 1089–1101.
12. Fourel, G., Revardel, E., Koering, C. E. & Gilson, E. (1999) *EMBO J.* **18**, 2522–2537.
13. Shei, G. J. & Broach, J. R. (1995) *Mol. Cell. Biol.* **15**, 3496–3506.
14. Chevallier, M. R., Bloch, J. C. & Lacroute, F. (1980) *Gene* **11**, 11–19.
15. Sikorski, R. & Hieter, P. (1989) *Genetics* **122**, 19–27.
16. Mahoney, D. J. & Broach, J. R. (1989) *Mol. Cell. Biol.* **9**, 4621–4630.
17. Holmes, S. & Broach, J. R. (1996) *Genes Dev.* **10**, 1021–1032.
18. Braunstein, M., Rose, A. B., Holmes, S. G., Allis, C. D. & Broach, J. R. (1993) *Genes Dev.* **7**, 592–604.
19. Boeke, J. D., Trueheart, J., Natsoulis, G. & Fink, G. R. (1987) *Methods Enzymol.* **154**, 164–175.
20. Gottschling, D. E., Aparicio, O. M., Billington, B. L. & Zakian, V. A. (1990) *Cell* **63**, 751–762.
21. Braunstein, M., Allis, C. D., Turner, B. M. & Broach, J. R. (1996) *Mol. Cell. Biol.* **16**, 4349–4356.
22. Feldman, J. B., Hicks, J. B. & Broach, J. R. (1984) *J. Mol. Biol.* **178**, 815–834.
23. Wright, J. H., Gottschling, D. E. & Zakian, V. A. (1992) *Genes Dev.* **6**, 197–210.
24. Loo, S. & Rine, J. (1994) *Science* **264**, 1768–1771.
25. Renauld, H., Aparicio, O. M., Zierath, P. D., Billington, B. L., Chhablani, S. K. & Gottschling, D. E. (1993) *Genes Dev.* **7**, 1133–1145.
26. Hecht, A., Laroche, T., Strahl-Bolsinger, S. & Grunstein, M. (1996) *Nature (London)* **383**, 92–96.
27. Pryde, F. E. & Louis, E. J. (1999) *EMBO J.* **18**, 2538–2550.
28. Boscheron, C., Maillet, L., Marcand, S., Trai-Pflugfelder, M., Gasser, S. & Gilson, E. (1996) *EMBO J.* **15**, 2184–2195.
29. Mahoney, D. J., Marquardt, R., Shei, G. J., Rose, A. B. & Broach, J. R. (1991) *Genes Dev.* **5**, 605–615.